The Curious Out-of-Plane Conductivity of PEDOT:PSS

*Kevin van de Ruit, Ilias Katsouras, Dirk Bollen, Ton van Mol, René A. J. Janssen, Dago M. de Leeuw, and Martijn Kemerink**

For its application as transparent conductor in light-emitting diodes and photovoltaic cells, both the in-plane and out-of-plane conductivity of PEDOT:PSS are important. However, studies into the conductivity of PEDOT:PSS rarely address the out-of-plane conductivity and those that do, report widely varying results. Here a systematic study of the out-of-plane charge transport in thin films of PEDOT:PSS with varying PSS content is presented. To this end, the PEDOT:PSS is enclosed in small interconnects between metallic contacts. An unexpected, but strong dependence of the conductivity on interconnect diameter is observed for PEDOT:PSS formulations without high boiling solvent. The change in conductivity correlates with a diameter dependent change in PEDOT:PSS layer thickness. It is suggested that the order of magnitude variation in out-of-plane conductivity with only a 3-4-fold layer thickness variation can quantitatively be explained on basis of a percolating cluster model.

1. Introduction

The conductive polyelectrolyte poly(3,4-ethylenedioxythiophene):poly(styrenesulfonate) (PEDOT:PSS) is commonly used as the transparent electrode in organic light-emitting diodes and in organic or hybrid photovoltaic cells. The chemical structures are presented in **Figure 1**a. In early applications, PEDOT:PSS was merely used for planarization and to stabilize the work-function of tin doped indium oxide (ITO). To prevent cross talk between neighboring pixels in display applications typically low conductivity PEDOT:PSS formulations were used, made by deliberately increasing the amount of PSS, so that only the out-of-plane conductivity was of importance. Recent efforts are aimed at fully replacing the expensive and brittle ITO layer with PEDOT:PSS.[1,2] This leads to the additional requirement of high in-plane conductivity to distribute the current across the device. This can be achieved by processing the colloidal dispersion with the addition of a high boiling solvent such as ethylene glycol, which is able to increase the in-plane conductivity of PEDOT:PSS to 1.4×10^5 S m^{-1}.[1]

Many studies have been performed in which the in-plane conductivity is addressed. However, in typical state of the art (organic) solar cells and light emitting diodes the main role of PEDOT:PSS is to transport charge in the out-of-plane direction. Nevertheless, only a few studies have been performed that measure the out-of-plane conductivity and they report widely varying results. Nardes et al.[3,4] found for PEDOT:PSS with a PEDOT:PSS ratio of 1:6 a large anisotropy in the in- and out-of-plane conductivity, roughly a factor 400, which was explained by the anisotropy in the granular structure as revealed by cross-sectional AFM. The out-of-plane conductivity was found to show an Arrhenius-type temperature dependence, while the in-plane conductivity showed a non-Arrhenius temperature dependence that could be explained using variable range hopping (VRH).[3,4] In studies towards self-assembled monolayer (SAM) electronics, van Hal et al.[5] found an anisotropy of 1000. Na et al.[6,7] have studied the influence of high boiling solvents on the conductivity using different techniques and found that adding different amounts of solvent can change the anisotropy from 7 to 50 and from 2000 to 30 000 for two different PEDOT:PSS formulations.

To gain understanding of the out-of-plane conductivity, we present a systematic investigation of the out-of-plane conductivity of PEDOT:PSS from a materials perspective. Unlike previous works we investigate a range PEDOT-to-PSS ratios. For comparison also a high-boiling solvent-treated PEDOT:PSS material is measured. A major problem in measuring the out-of-plane conductivity of highly conductive PEDOT:PSS formulations is that the thin film resistance easily drops below the contact resistance, hindering the acquisition of useful data. For the present PEDOT:PSS formulations this requires devices to have areas less than roughly 100 μm^2. Given the small layer thickness for spin-coated layers, i.e., ≈100 nm, even a modest out-of-plane conductivity, e.g., 1 S m^{-1}, can result in devices with very low resistance, i.e., 0.1 Ω for a 1 mm × 1 mm device. Since contact resistances are typically of the order 1–10 Ω, micrometer sized devices are required. Therefore, we use devices

K. van de Ruit, Prof. R. A. J. Janssen, Dr. M. Kemerink
Eindhoven University of Technology
Department of Applied Physics
P.O. Box 513, NL-5600 MB Eindhoven, The Netherlands
E-mail: m.kemerink@tue.nl
I. Katsouras
Zernike Institute for Advanced Materials
University of Groningen
Nijenborgh 4, NL-9747 AG, Groningen, The Netherlands
D. Bollen
Agfa-Gevaert N.V., Septestraat 27, 2640 Mortsel, Belgium
Dr. A. M. B. van Mol
Holst Centre/TNO
High Tech Campus 48, 5656 AE Eindhoven, The Netherlands
Prof. D. M. de Leeuw
Max Planck Institut für Polymerforschung
Ackermannweg 10, D-55128, Mainz, Germany

DOI: 10.1002/adfm.201301175

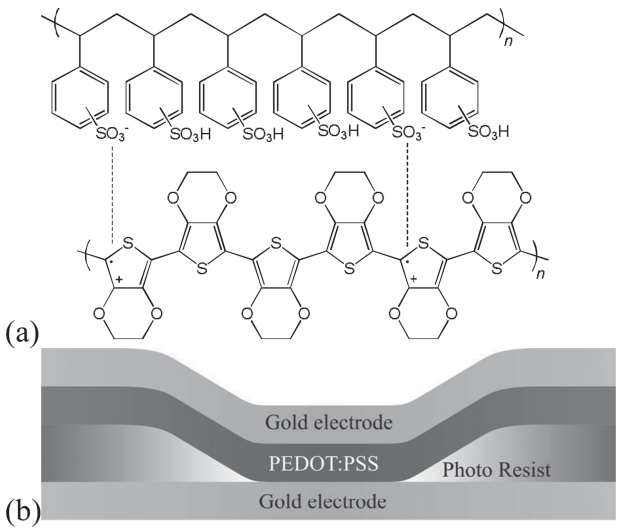

Figure 1. a) Schematic representation of the chemical structure of PEDOT:PSS. PEDOT (below) and PSS (top) bound via the Coulomb attraction between charged monomers of both macromolecules, indicated by the dashed line. b) Schematic representation of a vertical interconnect (via) used to measure the out-of-plane conductivity of PEDOT:PSS.

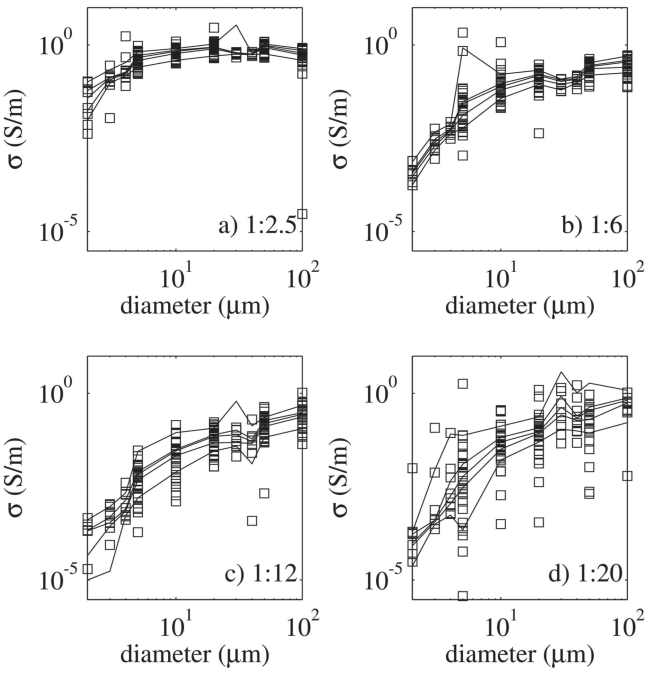

Figure 2. Measured conductivities for devices with PEDOT:PSS ratio 1:2.5, 1:6, 1:12 and 1:20. The solid lines indicate the 20%, 40%, 50%, 60%, and 80% percentiles (bottom to top) of the full dataset. Nominal PEDOT:PSS film thicknesses of a) 60 nm, b) 45 nm, c) 40 nm, and d) and 30 nm have been used in the conductivity calculation.

which consist of circular interconnects (vias) in an insulating photoresist layer sandwiched between two metallic electrodes, as shown in Figure 1b. Via diameters vary between 1 μm and 100 μm. A strong diameter dependence of the out-of plane conductivity is observed. Hence, the anisotropy of the conductivity is diameter dependent. For PEDOT:PSS formulations without high boiling solvent this dependence can amount to several orders of magnitude. These facts hint at the existence of a fundamental underlying mechanism. Unraveling this mechanism is the main topic of this article.

2. Results

A representative dataset of the measured out-of-plane conductivity as a function of via diameter for PEDOT:PSS in the ratios of 1:2.5, 1:6, 1:12 and 1:20 is presented in **Figure 2**. The complete dataset can be found in Supporting Information Figure S1. Since the highly conductive shorts fully determine the averages, percentiles have been studied instead. The five lines in each graph show for each diameter, from bottom to top, the 20%, 40%, 50%, 60%, and 80% percentiles of the complete set of all measured values. Remarkably, for all PEDOT:PSS ratios there remains a very strong trend in conductivity as a function of diameter that is larger than the typical spread between the 20% and 80% percentiles. Furthermore, there appears an increase in the scatter for devices with lower PEDOT:PSS ratio.

Figure 3a shows the median of the out-of-plane conductivity as a function of via diameter for PEDOT:PSS formulations in the ratios of 1:2.5, 1:6, 1:12, and 1:20. All devices consistently show an orders of magnitude decrease in conductivity with decreasing diameter. The devices can be divided into groups with similar conductivities. Since a physical interpretation is yet missing, these groups will be phenomenologically described by the function $\sigma \propto [\exp[(d_0/d)^{1/2}] + Rs]^{-1}$, where d_0 is a typical length scale and $Rs = 6\ \Omega$ is a series resistance accounting for the contact resistance between the Au and the PEDOT:PSS, the gold strips between the probe needles and the via, and the cabling. The first group, i.e., the devices with PEDOT:PSS ratio 1:2.5, is well described by the typical length scale $d_0 = 25$ μm indicated by the upper thick line. The second group, consisting of all other PEDOT:PSS ratios, i.e., 1:6, 1:12 and 1:20, seems well approximated by the lower thick line, following the same relation with $d_0 = 100$ μm, i.e., the diameter dependence is more pronounced than for 1:2.5. The near PEDOT:PSS ratio independence of the out-of-plane conductivity for ratios between 1:6 and 1:20 is in stark contrast to the in-plane conductivity that varies by almost two orders of magnitude over the same composition range, see **Figure 4**a.

For comparison the conductivity for the PEDOT:PSS type ICP 1020 with high boiling solvent has been measured. The result is shown in Figure 3b. The measured values are shown together with their percentiles. The spread in measurement values is very small. In contrast to the materials without high boiling solvent, the conductivity does not depend on diameter. The data can be fitted with a diameter independent conductivity of 10 S m^{-1}, taking into account a series resistance $Rs = 10\ \Omega$. Devices with a diameter of 2 μm, however, do not yield consistent results. The in-plane-conductivity is 3 10^4 S m^{-1} yielding an in-plane/out-of-plane anisotropy of 3200, independent of diameter.

The in-plane conductivity of spin coated films of the different PEDOT:PSS ratios is presented in Figure 4a as a

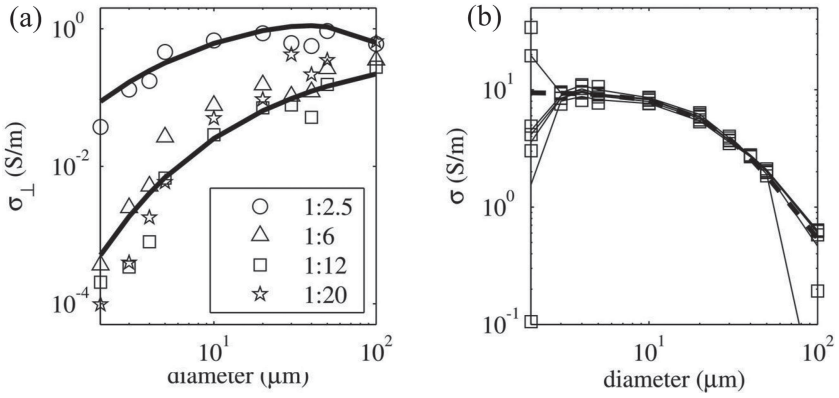

Figure 3. a) Median conductivities for devices with PEDOT:PSS ratio 1:2.5, 1:6, 1:12, and 1:20. The black thick lines are fits to the empirical relation discussed in the text, using a series resistance of 6 Ω. b) Measured conductivities (squares) for PEDOT:PSS of type 'ICP 1020' to which a high boiling solvent has been added. The solid lines indicate the 20%, 40%, 50%, 60%, and 80% percentiles. The thick dashed line is fitted using a diameter independent conductivity of 10 S m^{-1} and a series resistance of 10 Ω. Nominal PEDOT:PSS film thicknesses have been used in the conductivity calculations in panels (a) and (b).

function of PEDOT composition. The black line indicates the power law relation $\sigma(300K) \propto c^{3.5}{}_{PEDOT}$. This relation was shown before in ref. [8], where this relation was shown to stem from 3D percolation of quasi-1D filaments. From the measured in-plane conductivity $\sigma_{\parallel}$ and the median out-of-plane conductivities $\sigma_{\perp}$ (Figure 3a) we calculate the anisotropy. The numbers derived are presented in Figure 4b as a function of via diameter. Only at the largest diameters the values are somewhat affected by the series resistance, as reflected by the slight upturn for PEDOT:PSS 1:2.5. The observed range of anisotropies stretches over four orders of magnitude and covers all previously published anisotropy values.[3–7] In order to study the dependence of the anisotropy on the PEDOT:PSS ratio, the anisotropy vs. PEDOT concentration for devices with a diameter of 50 μm is shown in Figure 4c. For this diameter the trend in conductivity with diameter has largely settled, and contact resistance effects are small. The experimental data is phenomenologically described by $\sigma_{\parallel}/\sigma_{\perp} \propto c^{2.5}{}_{PEDOT}$, shown as the thick line in Figure 4c.

The diameter dependence of the conductivity and the anisotropy is very strong; both vary by nearly four orders of magnitude. Moreover, the variation is very similar for the PEDOT:PSS ratios 1:6, 1:12 and 1:20. These facts hint at the existence of a fundamental underlying mechanism. This mechanism will also have to explain the reduced diameter dependence for the ratio 1:2.5 and the lack of diameter dependence in the samples of PEDOT:PSS type ICP1020.

In addition to the conductivity and anisotropy dependence on diameter, our devices show a layer thickness dependence on diameter as well. To study and quantify this dependence, AFM measurements have been performed on finished devices, as shown in **Figure 5**. The inset in Figure 5a shows a topographic image of the top gold electrode of the device. In the middle of the image the via is visible as a depression, the depth of which is measured along the cross-section indicated by the white dotted line, and plotted in the main panel of Figure 5a. Considering the device layout shown in Figure 1b, the depth of the observed dip can directly be translated into (variations in) the PEDOT:PSS layer thickness inside the via provided the thickness of the photoresist layer (≈520 nm) and of the PEDOT:PSS layer outside the via (≈40 nm) are known.

To investigate the PEDOT:PSS layer thickness dependence on diameter, the depth of devices for PEDOT:PSS in the ratios 1:6, 1:12 and 1:20 is shown in Figure 5b. Figure 5c,d shows the same for PEDOT:PSS in the ratio 1:2.5 and for PEDOT:PSS type ICP1020, respectively. For Figure 5b,c there is a decrease in depth with decreasing diameter, which can be related to an increase in PEDOT:PSS layer thickness. An alternative explanation could be that there is a systematic change of photoresist layer thickness with device diameter. To avoid such systematic errors, we measured devices both at the center and at the edge of the substrate; thereby the influence of systematic thickness variations of the photo resist layer is ruled out. Alternative scenarios that might give rise to an apparent diameter dependent layer thickness like shadow effects during the gold evaporation or photo resist thickness variations related to the etching of the vias can be ruled out since they would equally affect all devices in Figures 5b–d, which is clearly not the case. We therefore attribute the observed depth variations to variations in PEDOT:PSS layer thickness in the vias, most likely caused by a diameter- and material-dependent interplay between viscosity, surface tension and contact-line pinning during the spin coating.

Summarizing the data in Figures 3–5, for the PEDOT:PSS formulations without high boiling solvent there is a significant diameter

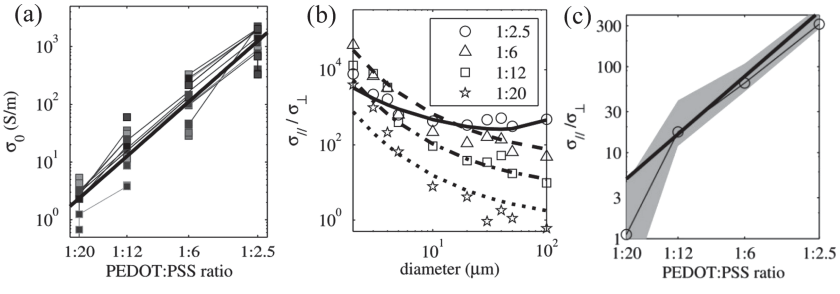

Figure 4. a) Double logarithmic plot of the room temperature in-plane conductivity vs. the PEDOT:PSS ratio. The black line indicates a power law relation with power 3.5 as a function of the PEDOT concentration. b) Symbols: Measured in-plane/out-of-plane anisotropies in the conductivity based on Figure 3a and panel (a). The continuous, dashed, dash-dotted and dotted lines indicate the anisotropies based on the empirical relations shown in Figure 3a for devices with PEDOT:PSS ratio 1:2.5, 1:6, 1:12 and 1:20 respectively. c) Double logarithmic plot of the measured median anisotropies for a via diameter of 50 μm vs. the PEDOT:PSS ratio (connected circles). The gray patch indicates the region between the 20% and 80% percentile of the data. The thick solid line indicates a power law dependence with exponent 2.5.

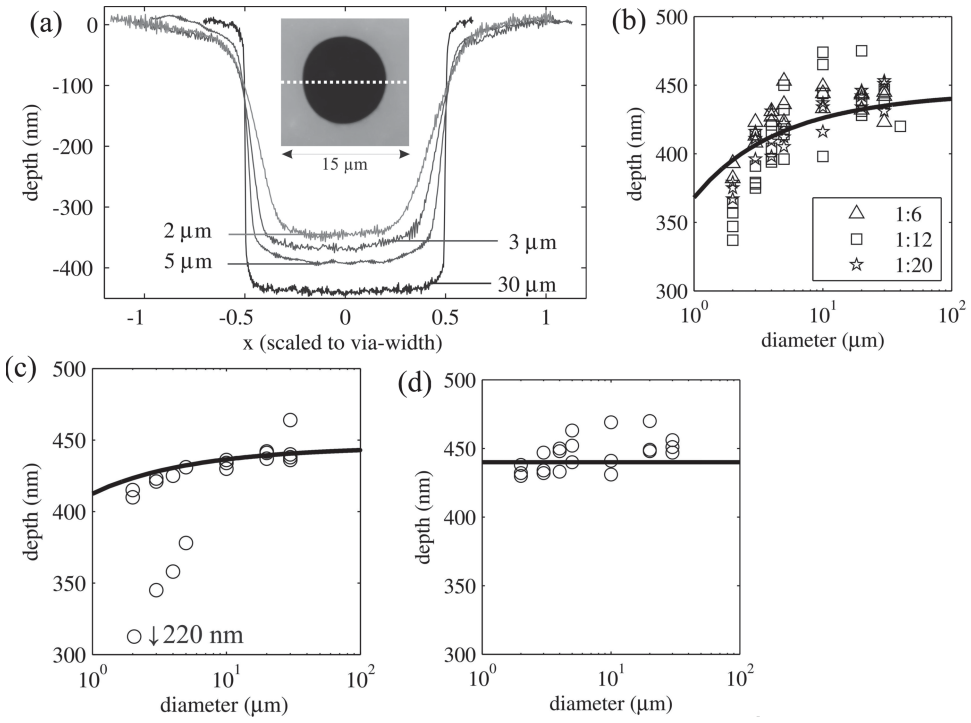

Figure 5. a) Inset: a topographic AFM image of a 10 µm device. The dashed white line indicates the typical location for the cross-sections shown in the main panel. The cross-sections are shown to the scale of the device-width and are measured on a substrate with PEDOT:PSS ratio 1:12. b–d) Depths determined by cross-sections as shown in (a) for (b) PEDOT:PSS with ratios 1:6, 1:12 and 1:20, c) PEDOT:PSS of ratio 1:2.5 and d) PEDOT:PSS type 'ICP1020'. Lines are calculated from Equation (1).

dependence both in the conductivity and in the PEDOT:PSS layer thickness. As such, also the conductivity anisotropy is diameter dependent. In principle, these dependencies may result from different mechanisms. However, there is a clear correlation between the degree of thickness variation and the degree of conductivity variation: the PEDOT:PSS formulations that give rise to the strongest thickness variation, i.e., 1:6, 1:12, and 1:20, also show the most pronounced conductivity variation. The ICP 1020 material shows neither a thickness nor a conductivity variation. The 1:2.5 material lays in between, both in thickness and in conductivity variation. This strongly suggests that there is a causal relation between thickness and out-of-plane conductivity. However, for a homogeneous Ohmic conductor a 3–4-fold layer thickness variation should not lead to a conductivity variation by several orders of magnitude. In the next section we suggest an interpretation of this surprisingly strong dependence of conductivity on diameter.

3. Discussion

Our experimental data shows that for certain PEDOT:PSS formulations both the thickness of the layer and its out-of-plane conductivity are dependent on the device diameter. To explain these experimental observations, several scenarios, such as highly conductive filaments, charge transport in a layered morphology, phase separation between PEDOT-rich and PSS-rich material and a PSS top layer model have been considered (see Supporting Information Section S3). All aforementioned models treat the observed dependencies as coexistent but without causal relation. We seek, however, a model that provides a link between the layers' thickness and the conductivity (anisotropy), as our data suggests. To that end, we make use of percolation theory.

3.1. Percolating Cluster Model

From our detailed analysis of the field, temperature and composition dependence of the in-plane conductivity we know that the thin layers of the PEDOT:PSS formulations without high boiling solvent are percolating systems of quasi-1D filaments near the percolation threshold.[8] In a broader perspective, percolation is typically a necessary ingredient for the interpretation of transport results in PEDOT:PSS.[3,4,8–11] This powerful theory describes the formation of connected, i.e., conductive, networks when conductive elements are successively added to an insulating matrix.[12] Most notably, the theory predicts that there exists a percolation threshold, i.e., a specific density of conductive elements beyond which macroscopic conduction occurs. Only above the percolation threshold does the system contain a connected network of infinite size. In concentrations close to the percolation threshold the system is in a critical regime, which means that a power law dependence on (changes in) the concentration of conductive elements occurs for many observables of the system, such as the conductivity or the probability of finding clusters of a particular size. Applying percolation theory to thin layers is difficult, since these layers are neither

two dimensional nor three dimensional. Instead, a cross-over is expected to occur with increasing layer thickness.[13,14] For the out-of-plane conductivity this means that the connected network responsible for conduction no longer needs to be infinitely large, but needs merely to have a size equal to the thickness of the layer. Early work uncovered interesting phenomena for such thin percolating systems, such as the following dependence of the out-of-plane conductivity on layer thickness:[14–16]

$$\sigma_{\perp} \propto \exp\left[-(44.6L/\xi)^{1/2}\right] \quad (1)$$

where L denotes the layer thickness, and ξ denotes the localization length, i.e., the length scale of the exponential decay of the localized electronic states. This equation reflects the fact that the probability of finding clusters with a size of at least the film thickness, i.e., that connect the electrodes, strongly decays with increasing thickness. Equation (1) holds for thin layers, i.e., small values of L/ξ. However, in ref. [14], good agreement between experiment and theory is reached even for $L/\xi \approx 300$. In ref. [8] the localization length for the present PEDOT:PSS emulsions has been determined to be $\xi = 10$ nm, whereas the layer thickness here varies between ≈40 nm and ≈140 nm. Although relation (1) has been derived for variable range hopping (VRH) in an isotropic system, similar relations are expected for the conductivity of the PEDOT:PSS films studied here, where the conductivity is determined by percolation through a 3D network of quasi-1D filaments.[8] Therefore, a strong dependence of the conductivity on layer thickness, such as described by Equation (1), does not require, nor imply, that hopping-type processes dominate the out-of-plane conductivity of PEDOT:PSS.

3.2. Diameter Dependent Thickness and Conductivity

In order to test whether thickness dependent percolation can explain our data, we have used Equation (1) to calculate the layer thickness from the conductivity. To this end, we take the empirically fitted conductivities in Figure 3 (thick continuous in panel (a) and thick dashed lines in panel (b)) and the previously determined $\xi = 10$ nm as input to calculate an estimate for L, and concomitantly for the apparent via depth. Additionally the following estimates have been made: the layer thickness for a diameter of 100 µm is 40 nm, i.e., the layer thickness on glass substrates using the same spincoating conditions, and the layer thickness of the photo resist layer is 520 nm. The results are shown as the black lines in Figure 5b–d. Given the fact that Equation (1) is used without any adjustments, the agreement with the measured depths is surprisingly good. Although the prediction shown by the black line somewhat underestimates the measured depths, the trend of increasing depth, and therefore decreasing PEDOT:PSS layer thickness, with increasing diameter is well reproduced in Figure 5b–d. Note that also the correlation between the degree of thickness variation and the degree of conductivity variation follows naturally from the model, as shown by the black lines in panels c and d. The percolation cluster model accounts for the reduced diameter dependence for the ratio 1:2.5 and the lack of diameter dependence in the samples of PEDOT:PSS type ICP1020.

3.3. Anisotropy

For the present PEDOT:PSS system a power law relation is found between the in-plane conductivity prefactor vs. PEDOT concentration, i.e., $\sigma_0 \propto c^{3.5}{}_{\mathrm{PEDOT}}$, with $\sigma_{\parallel} = \sigma_0 f(T)$ where $f(T)$ accounts for the temperature dependence of the in-plane conductivity. The power law dependence on concentration has been explained in the context of the critical regime near the percolation threshold.[8] The interpretation of the conductivity dependence on layer thickness as a result of the percolative nature of conduction in PEDOT:PSS is also in accordance with the decreasing anisotropy with decreasing PEDOT concentration shown in Figure 4c. That is, at lower PEDOT concentrations, small connected clusters have a lower probability of contributing to the in-plane conductivity, but have a similar probability of contributing to the out-of-plane conductivity due to the thinness of the film. This causes the out-of-plane conductivity to be approximately linear with PEDOT concentration. Since the in-plane conductivity depends on the PEDOT concentration as $\sigma_0 \propto c^{3.5}{}_{\mathrm{PEDOT}}$, this combines into an anticipated power-law dependence of the anisotropy $\sigma_{\parallel}/\sigma_{\perp} \propto c^{2.5}{}_{\mathrm{PEDOT}}$. This result explains well the trend in the measured anisotropies as shown in Figure 4c by the solid black line.

One aspect of the anisotropies remains to be clarified, namely the fact that $\sigma_{\parallel}/\sigma_{\perp} > 1$. This seems in contradiction to the statement above that clusters that do not contribute to the in-plane conductivity can still contribute to the out-of-plane conductivity, which would result in $\sigma_{\parallel}/\sigma_{\perp} < 1$. This requires that the clusters themselves are inherently anisotropic. Such an inherent anisotropy naturally arises when the filaments in the PEDOT:PSS layer, observed in ref. [8], are predominantly oriented in-plane, causing out-of-plane conduction paths to have a zigzag pattern. Considering that the length of the filaments of approximately 100 nm is larger than the layer thickness, it is highly likely that the filaments indeed have a preferential in-plane orientation.

4. Conclusions

The out-of-plane conductivity of thin films of PEDOT:PSS (without high boiling solvent) for varying PEDOT contents has been systematically investigated using devices consisting of circular vias with varying diameter. This reveals a strong and significant diameter dependence of the median out-of-plane conductivity over more than three orders of magnitude. At large diameters, where this diameter dependence levels off, comparison to the in-plane conductivity shows an orders of magnitude change in anisotropy with PEDOT:PSS ratio.

To investigate the trends in conductivity and anisotropy with via diameter, several models have been tested and rejected. The behavior can be well explained in the context of percolating clusters, the abundance of which strongly decreases with size. The strong diameter dependence of the conductivity can quantitatively be explained by a concomitant change in layer thickness: it reflects the fact that the probability of finding clusters with a size of at least the film thickness, i.e., that connect the electrodes, strongly decays with increasing thickness. This theoretical framework is also fully consistent with the trend found

in the anisotropy by varying the PEDOT:PSS ratio. Increasing the PEDOT:PSS ratio strongly increases the abundance of clusters contributing to the in-plane conductivity, while only marginally increasing the number of clusters contributing to the out-of-plane conductivity.

The presented strong dependence of out-of-plane conductivity on layer thickness is of evident relevance to applications which typically require a minimum value for the out-of-plane conductivity of PEDOT:PSS. Examples are the application of PEDOT:PSS in hole-extracting contacts or recombination layers in (tandem) solar cells or in the anode of OLEDs. This interpretation also rationalizes previously unexplained findings in molecular junctions where PEDOT:PSS is used as contact electrode.

5. Experimental Section

PEDOT:PSS emulsions were obtained from AGFA-GEVAERTS N.V. The emulsion used to prepare the samples is PEDOT:PSS ratio 1:2.5, named 'generation 5', and is commercially available as ICP-1050. PEDOT:PSS ratios 1:6, 1:12, and 1:20 were prepared using the stock dispersion of PEDOT:PSS in ratio 1:2.5. The PEDOT:PSS ratio was adapted by adding PSS. Where necessary, water was added to obtain a solid content of (0.90 ± 0.04) wt%. To obtain homogeneous emulsions we sonified the solutions. This procedure for preparing the emulsions is the same as used in ref. [8]. Additionally, as a reference sample, the commercially available PEDOT:PSS material ICP-1020, from the same manufacturer has been used. To this sample 5 vol% dimethyl sulfoxide (DMSO) was added as a high boiling point solvent.

The out-of-plane conductivity measurements of PEDOT:PSS were performed using the previously developed technology of large-area molecular junctions. The devices were prepared according to the procedures described elsewhere.[17] Two types of junctions were prepared that differed only in the used photoresist; the measurement results were completely consistent. As substrates a 4" or 6" silicon wafer with a 500 nm thermally grown silicon oxide was used. On this wafer, a 1 nm layer of chromium was thermally evaporated through a shadow mask, followed by 60 nm of gold. The RMS roughness of the bottom contact is about 0.7 nm over an area of 0.25 μm^2. The via in each two terminal junction was photolithographically defined in an insulating matrix of photoresist, either ma-N 1410 or L6000.5 (Micro Resist Technology GmbH) that was deposited by spin coating. After a pre-bake step to remove any remaining solvents, the layer was exposed to UV light with a Karl Süss MA1006 mask aligner, to define the vertical interconnects, 'vias', with diameters ranging from 1 to 100 µm. Unfortunately devices with a diameter of 1 µm were of a low quality, resulting in too much scatter to be included in the analysis. After development, the film was hard baked at 200 °C for at least 1h. The wafer was subsequently cut in several pieces. This allowed the simultaneous processing of different PEDOT:PSS compositions on a single wafer, thereby eliminating processing variations that can affect device performance. A last step before PEDOT:PSS deposition was cleaning of the bottom gold contacts with a PDC plasma cleaner (Harrick plasma) to remove any photoresist residuals. To obtain an equal layer thickness for all PEDOT:PSS of varying ratio, the following spin coat parameters were used. The ramp-rate was 1000 RPM s^{-1} and the first spincoating step is 500 RPM for 5 s followed by 120 s of 2000 RPM (for 1:2.5), 1700 RPM (1:6), 1500 RPM (1:12), 1500 RPM (1:20), or 1500 RPM (ICP1020). On planar test substrates these parameters led to layer thicknesses around 40 nm for PEDOT:PSS ratios 1:2.5, 1:6, 1:12, and 1:20 and to a thickness of around 100 nm for the ICP 1020. After spincoating, the wafer was then immediately transferred to a vacuum oven for at least 1 h to dry the film. As top electrode, 100 nm of gold was evaporated through a shadow mask. This gold layer, apart from providing electrical contact with the measurement probes, also serves as a self-aligned mask for the removal of redundant PEDOT:PSS by reactive ion etching (O_2 plasma). This step eliminates any parasitic currents from top to bottom electrode.

For the in-plane conductivity measurements substrates were used that consisted of 3 cm × 3 cm bare sodalime glass. They were first grooved into small pieces of 1 cm × 1 cm on the back side with a diamond pen, then sonicated in a bath of acetone for 10 min, cleaned with soap, rinsed with deionized water for 20 min and sonicated in a bath of iso-propanol for 10 min. Residual organic contaminations were removed using a 30 min. UV-ozone treatment (UV-Ozone Photoreactor, PR-100, Ultraviolet Products).

The PEDOT:PSS solutions were filtered using a 0.5 µm filter and deposited in air by spin coating at 1000 RPM for 1 min, followed by 3000 RPM for 1 min to dry the layer. This typically resulted in layer thicknesses of 60 nm, 45 nm, 40 nm, and 30 nm PEDOT:PSS in ratio of 1:2.5, 1:6, 1:12, and 1:20, respectively. After spin coating, samples were transferred into a glove box (O_2 and H_20 < 1 ppm) and subsequently annealed on a hot plate at 200 °C for a few minutes to remove residual water. Four electrodes (1 mm × 8 mm, 1 mm apart from each other) of 100 nm of gold were evaporated on top of each 1 cm × 1 cm piece.

After breaking the desired sample from the substrate, it was placed inside a cryostat (Oxford Instruments, modified for reaching low pressures) and evacuated to pressures below 10^{-6} mbar. The samples were exposed to air for a few minutes between the removal form the glove box and insertion into the cryostat. It was found that the room temperature conductivity only changes after exposure to air for a few hours. Once placed, samples were degassed at 200 °C for a few hours to reach low pressures. This annealing step in vacuum did not alter the room temperature conductivity.

The two point probe in-plane conductivity and out-of-plane conductivity measurements were performed as bias sweeps between –0.5 V and 0.5 V using a Keithley 2636a source-measure unit. To avoid the influence of water on the conductivity of PEDOT:PSS, exposure of the samples to air was minimized and electrical measurements were performed in a glovebox. The conductivities reported in this article are the conductivities measured at a bias at 0.5 V. The bias dependence of the conductivity is shown in the Supporting Information Figure S2.

Supporting Information

Supporting Information is available from the Wiley Online Library or from the author.

Received: April 5, 2013
Published online: June 19, 2013

[1] Y. H. Kim, C. Sachse, M. L. Machala, C. May, L. Müller-Meskamp, K. Leo, *Adv. Funct. Mater.* **2011**, *21*, 1076.
[2] Y. Xia, K. Sun, J. Ouyang, *Adv. Mater.* **2012**, *24*, 2436.
[3] A. M. Nardes, M. Kemerink, R. A. J. Janssen, *Phys. Rev. B* **2007**, *76*, 085208.
[4] A. M. Nardes, M. Kemerink, R. A. J. Janssen, J. A. M. Bastiaansen, N. M. M. Kiggen, B. M. W. Langeveld, A. J. J. M. van Breemen, M. M. de Kok, *Adv. Mater.* **2007**, *19*, 1196.
[5] P. A. van Hal, E. C. P. Smits, T. C. T. Geuns, H. B. Akkerman, B. C. D. Brito, S. Perissinotto, G. Lanzani, A. J. Kronemeijer, V. Geskin, J. Cornil, P. W. M. Blom, B. D. Boer, D. M. de Leeuw, *Nat. Nanotechnol.* **2008**, *3*, 749.
[6] J.-S. Yeo, J.-M. Yun, D.-Y. Kim, S. Park, S.-S. Kim, M.-H. Yoon, T.-W. Kim, S.-I. Na, *ACS Appl. Mater. Interfaces* **2012**, *4*, 2551.
[7] S.-I. Na, G. Wang, S.-S. Kim, T.-W. Kim, S.-H. Oh, B.-K. Yu, T. Lee, D.-Y. Kim, *J. Mater. Chem.* **2009**, *19*, 9045.

[8] K. van de Ruit, R. Itzhak, D. Bollen, A. M. B. van Mol, R. Yerushalmi–Rozen, R. A. J. Janssen, M. Kemerink, unpublished.
[9] C. S. Suchand Sangeeth, M. Jaiswal, R. Menon, *J. Phys. Condens. Matter* **2009**, *21*, 072101.
[10] J. Ouyang, Q. Xu, C.-W. Chu, Y. Yang, G. Li, J. Shinar, *Polymer* **2004**, *45*, 8443.
[11] S. Samitsu, T. Shimomura, K. Ito, M. Fujimori, S. Heike, T. Hashizume, *Appl. Phys. Lett.* **2005**, *86*, 233103.
[12] Y. P. Mamunya, *J. Macromol. Sci., B* **1999**, *38*, 615.
[13] B. I. Shklovskii, A. L. Efros, *Electronic Properties of Doped Semiconductors*, Springer Verlag, Heidelberg **1984**.
[14] M. Pollak, J. J. Hauser, *Phys. Rev. Lett.* **1973**, *31*, 1304.
[15] A. V. Tartakovskii, M. V. Fistul', M. E. Raikh, I. M. Ruzin, *Sov. Phys. Semicond.* **1987**, *21*, 603.
[16] vA near literal copy of Reference [16] is available online as Y. Park, *Solid State Commun.* **2000**, *115*, 281.
[17] I. Katsouras, V. Geskin, A. J. Kronemeijer, P. W. M. Blom, D. M. de Leeuw, *Org. Electron.* **2011**, *12*, 857.